

Article

Modeling and Analysis of Current Loading Effects on Electric Vehicle's Lithium-Ion Batteries: A MATLAB-Based Model Approach

Oladipo Folorunso ^{1,2,*}, Rotimi Sadiku ^{1,3}, Yskandar Hamam ^{2,4} and Williams Kupolati ⁵

¹ Department of Chemical, Metallurgical, and Materials Engineering, Tshwane University of Technology, Pretoria 0001, South Africa; sadikur@tut.ac.za

² French South African Institute of Technology (F'SATI)/Department of Electrical Engineering, Tshwane University of Technology, Pretoria 0001, South Africa; hamama@tut.ac.za

³ Institute of NanoEngineering Research (INER)/Department of Chemical, Metallurgy and Material Engineering, Tshwane University of Technology, Pretoria 0001, South Africa

⁴ École Supérieure d'Ingénieurs en Électrotechnique et Électronique, Cité Descartes, 2 Boulevard Blaise Pascal, Noisy-le-Grand, 93160 Paris, France

⁵ Department of Civil Engineering, Tshwane University of Technology, Pretoria 0001, South Africa; kupolatiwk@tut.ac.za

* Correspondence: folorunsoo@tut.ac.za

Abstract: Beyond portable mobile devices, lithium-ion batteries play a crucial role in electric vehicle operations and stationary grid power generation. However, the aging of lithium-ion batteries, often accelerated by extreme temperatures and load current influences, requires thorough examination and solution. The high load current, cycling, temperature differential, and operational conditions are factors contributing to the reduction in capacity and shortened lifespan of lithium-ion batteries. In this study, a lithium-ion ($\text{LiNi}_x\text{Mn}_y\text{Co}_z\text{O}_2$) battery was modeled by using the MATLAB/Simulink model technique. In order to investigate the effect of resistance build-up in the batteries, the capacity of the batteries (old and new batteries) was analyzed over different usage periods: 360 cycles, 1000 cycles, and 2000 cycles. A cooling system was introduced to explicitly carry out an inductive analysis of the effect of temperature on the performances of the batteries. The effect of load current on the capacity of the battery was examined between 30 A and 100 A. The results showed that the available capacity of a battery is proportional to its usage rate. Generally, when the load current on the batteries (old and new batteries) was 30 A, the battery was ideally in good health even after 1000 cycles for a 2 h discharge time. In addition, the old battery, however, showed a capacity decrease to about 74.15% and 74.94% for scenarios 1 and 2 after 1000 cycles for a 2 h discharge time when the batteries were subjected to a 100 A discharge current. Amongst other factors, scenarios 1 and 2 can be differentiated by whether the battery pack discharges uniformly or non-uniformly, whether the individual cells operate under the same or different discharge cycles, and whether the batteries are with cooling or without a cooling system. The voltage and temperature differences between the old and new batteries, after 2000 cycles for the 100 A load current, are 4.0 V and 5.3 °C (scenario 2), respectively. Moreover, after 360 cycles at a 100 A discharge current, the temperature difference between the old and new batteries was 4.5 °C in scenario 1 and 2.3 °C in scenario 2. Based on the results obtained in this study, useful equations for proper calibration, voltage, and cooling switching time characteristics were proposed. Additionally, the study results indicated that at higher load currents, battery degradation became less affected by temperature differentials. The results of this study will aid in the adequate load optimization and thermal management of lithium-ion batteries for electric vehicle applications.



Citation: Folorunso, O.; Sadiku, R.; Hamam, Y.; Kupolati, W. Modeling and Analysis of Current Loading Effects on Electric Vehicle's Lithium-Ion Batteries: A MATLAB-Based Model Approach. *Batteries* **2024**, *10*, 417. <https://doi.org/10.3390/batteries10120417>

Academic Editor: Rodolfo Dufo-López

Received: 10 September 2024

Revised: 5 November 2024

Accepted: 26 November 2024

Published: 27 November 2024



Copyright: © 2024 by the authors. Licensee MDPI, Basel, Switzerland. This article is an open access article distributed under the terms and conditions of the Creative Commons Attribution (CC BY) license (<https://creativecommons.org/licenses/by/4.0/>).

Keywords: electric vehicles; lithium ion; model; current; battery; global warming

1. Introduction

The adoption of electric vehicles offers numerous advantages, including reduced environmental pollution, economic growth, and simplified transportation. These benefits are significant, and they correlate with the growing global market for electric vehicles [1]. Therefore, the increase in production, adoption, and utilization of electric vehicles can significantly enhance the mitigation of the greenhouse gas threat [2]. However, to make electric vehicles viable alternatives to internal combustion vehicles, advancements in efficient battery development and proper battery thermal management are essential [3]. An electric vehicle's efficient operation is a function of the source of storage energy, the power needed, and the braking need. The absorber of the electromechanical energy losses in electric vehicles is the energy source (i.e., the battery and supercapacitor). The losses from the various components of electric vehicles, such as variable- and constant-speed drives, gears, and power converters, contribute to the rapid aging of electric vehicle batteries [4].

The lithium-ion battery pack is the most prominent component of modern electric vehicles. In fact, lithium-ion batteries have no memory effect; they are lightweight, and they possess high energy density [5,6]. Nevertheless, lithium-ion battery performance is still faced with several challenges, such as capacity fade, poor power density, cycling, and electrode cracking [7]. Lithium-ion batteries' cycling and cracking problems can be attributed to the temperature differential in the battery cells [8]. Therefore, the sensitivity of the battery to temperature changes must be thoroughly examined and addressed. This will enable the proper battery thermal management and usage within a desirable thermal change window.

Chen et al. [9] reported that the cooling of lithium-ion batteries for electric vehicles is crucial to keep the battery temperature within a 15 °C and 35 °C thermal change. The battery safety, end of life, and cost are expected to improve at optimized operating temperatures. For all kinds of driving conditions, especially in aggressive driving situations, the cells of lithium-ion batteries must be maintained within a specific operating temperature range and uniformity [10].

The study of lithium-ion battery performance in relation to temperature impact, charge/discharge rates, and aging cannot be overstated. This factor requires a thorough examination to ensure sustainable and efficient electric vehicle utilization. From the study conducted by Moayedi [11] on the performance improvement and thermal management of a lithium-ion battery, through tab locations and cell aspect ratio optimization, Moayedi concluded that the tab location and aspect ratio of lithium-ion battery cells have a significant influence on the temperature distribution within the battery. A maximum reduction in the build-up temperature within a lithium-ion battery can be achieved through an optimized aspect ratio, as well as the use of counter and L-shape tabs of the battery cells. Battery charge and discharge performance is generally affected by temperature, whether in cold or hot climates. Hence, the battery must be optimally operated at the designed temperature range, regardless of the internally generated heat and the ambient temperature. At very low temperatures, lithium-ion battery capacity tends to degrade due to the low lithium-ion diffusion rate. Another effect that often results from a low working temperature of lithium-ion batteries is the lithium plating on the electrode surface. The very low operating temperatures will result in low charge-transfer velocity and will invariably decrease the ionic conductivity of the battery electrolytes and the battery capacity due to the low lithium-ion diffusivity tendency [12].

Jiang et al. [13] experimentally and theoretically investigated the desirable preheating method of lithium-ion batteries in cold climates. In the study, the effect of preheating of lithium-ion batteries was investigated with respect to the metal resistance film and the inductive heating methods. Owing to the uniform temperature distribution and the high efficiency of the battery, Jiang et al. reported that inductive heating is a better preheating method in cold climates. The factors on which the inductive heating method relies include the battery thickness and the current frequency. The environmental temperature effects, in addition to the usage condition of the lithium-ion batteries, determine the effective

temperature of the battery cells. Therefore, the battery temperature is the total internal temperature of the cells, which may depend on several factors, such as the charge and discharge current rate and external temperature [14]. In addition, the battery's internal resistance will increase at low working temperatures, leading to increased power loss [15].

High charge and discharge current rates, deep discharge states, and high or low operating temperatures of lithium-ion batteries are detrimental to the cycle life, capacity, and efficiency of lithium-ion batteries. The relationship between the battery current and temperature can be described as shown in Equation (1) [16].

$$I_{batt} \approx \exp\left(-\left(\frac{1}{T_{batt}}\right)\right) \quad (1)$$

where I_{batt} and T_{batt} are the battery current and temperature. A lithium-ion battery can age quickly when it is continuously subjected to temperatures that are above its optimal temperature limit. High operating temperature is associated with changes in the electrode binders and the solid electrolyte interface. These changes have effects on the battery's impedance [12]. For instance, the freezing of the battery causes a high power loss, while overheating of the battery causes a reduction in the life cycle and capacity of the batteries. Hence, the importance of battery thermal management, in this case, the activation of heaters and coolers when necessary, is significant for ensuring reliability, safety, cost-efficiency, and a long lifespan for electric vehicle batteries [14]. Table 1 provides the primary causes of battery capacity/power fades and their formation mechanisms.

Table 1. Causes of battery aging and their formation mechanisms [17,18].

Causes	Cycling	High temperature	High cell voltage	Load current	Mechanical stress	Low temperature	Low cell voltage
Mechanisms	Solid electrolyte interface	Solid electrolyte interface, cathode electrolyte interface, decomposition of electrolyte, binder decomposition, transition metal dissolution	Solid electrolyte interface, decomposition of electrolyte, binder decomposition, graphite exfoliation, corrosion of current collector	Solid electrolyte interface, decomposition of electrolyte, graphite exfoliation, lithium plating, structural disordering, electrode cracking	Solid electrolyte interface, structural disordering, electrode cracking	Lithium plating	Lithium plating, transition metal dissolution, and current collector corrosion
Degradation modes	Loss of lithium inventory		Loss of active materials			Conductivity loss	
	Solid electrolyte interface, cathode electrolyte interface, decomposition of electrolyte, lithium plating		Solid electrolyte interface, cathode electrolyte interface, graphite exfoliation, lithium plating, structural disordering, electrode cracking, transition metal dissolution			Binder decomposition, graphite exfoliation, structural disordering, electrode cracking, current collector corrosion	
Effects	Capacity fade		Capacity fades, and power fade			Power fade	

As observed in Table 1, load current causes solid electrolyte interface formation, electrolyte decomposition, graphite exfoliation, lithium plating, structural disordering, and cracking and fracturing of the lithium-ion battery electrodes. That is, the load current is another critical aging factor in lithium-ion batteries. A solid electrolyte interface is a passivating layer on the anode of a lithium-ion battery, formed as a result of the electrolyte decomposition at the surface of the battery anode electrode [19]. Solid electrolyte interface affects the performance, capacity, and battery safety [20]. Besides the low-temperature effect, lithium plating (metallic lithium, formed on the anode of a lithium-ion battery), occurs due to the high discharging and charging current, a high state of charging, and capacity imbalance [21].

Moreover, when the load current increases, the battery's operating temperature tends to rise, giving rise to the electrode material volume change. The resulting thermal stress, due to the electrode material volume change, can lead to the cracking and fracturing of the electrodes. The cracking and fracturing of electrode materials has a major effect on the electrical and ionic conductivities of the battery, due to the disruption of electrical contact between the current collector, and the conductive additives/active particles [22].

The electric vehicle sensitivity to battery performance requires an accurate analysis of the battery aging. Therefore, modeling battery characteristics is essential for their optimal usage. In the literature, physicochemical and artificial neural network models have been proposed to characterize the aging behaviors of batteries [23,24]. Li et al. [25] combined the electrothermal model with an artificial neural network to analyze the efficiency of a cooling system on battery aging. Li et al. concluded that the coupled model is an efficient optimization tool for investigating the cooling effects on battery performance. However, the coupled model is short of many parameters, such as the number of cells, electrode materials, and many other factors. Hahn et al. [26] reported that although the various existing theoretical models are optimistic modeling approaches, they lack parameters that can describe the aging of batteries.

Extensive research has been conducted on the thermal management of batteries. Nevertheless, the consequential effects of load current on the degradation of lithium-ion batteries have not been fully explored. Therefore, considering the impacts of load current on the lifespan of batteries for electric vehicles, this study focuses on modeling the effects of load current on lithium-ion battery aging using MATLAB/Simulink (9.14.0.2286388 (R2023a) Update 3). This study compares the performances of old and new batteries, taking into consideration the cooling effect. MATLAB/Simulink software [27] is versatile, simple to use, and efficient in designing battery packs and characterizing batteries for real-life scenarios. Table 2 presents the concept of this study.

Table 2. Study concept.

Concepts	Questions
Load current	How do different load currents affect the capacities of old and new batteries?
Temperature	Can temperature be the predominant factor negatively influencing battery life cycles?
Cycle life	How does cycle life impact battery performance?
Module and assembly discharge cycles	Does imbalance discharge across cells affect the overall performance and reliability of battery packs?
Module and assembly thermal resistance	Can the effect of non-uniform thermal resistance within battery packs impact battery life cycles?

Furthermore, this study aims to further explore the battery thermal management scheme from the perspective of load current and cooling performances of lithium-ion batteries. The choice of MATLAB for this investigation is due to its flexibility, ease of use, availability of specialized toolboxes, and built-in functions for battery thermal management analysis and the robustness of the Simulink/SIMSCAPE package. Section 2 of this study succinctly provides this study's methodology. Two different batteries were modeled, namely the old and new batteries. In addition to these two groups of batteries, two scenarios were assumed. In scenario 1, the batteries were studied with and without the influence of coolant, and the cells were subjected to non-uniform discharge. In scenario 2, the batteries were studied by considering the influence of coolant and the possibility of uniform discharge. An important observation from the simulation results is that, at very high load currents, the degradation of the battery is less influenced by the associated thermal changes. While thermal management is crucial for maintaining battery performance and longevity, the contribution of extremely high current demands to the temperature differential must

also be a priority concern. In other words, under normal and moderate load conditions, battery thermal management helps prevent overheating and ensures efficient operation. However, the main causes of battery degradation shift when the battery is subjected to extremely high current demands. This insight highlights the need to consider a range of operational scenarios when designing battery management systems, and it underscores the importance of addressing other forms of stress that batteries encounter under high-load currents in order to ensure their durability and efficiency. The results and discussion are presented in Section 4. Further discussion and validation of the results are provided in Section 4.3, while Section 5 gives the conclusion of this study.

2. The Modeling Methodology

Battery degradation can be noticed from the energy capacity loss and the decrease in the power output of the cells [28]. Various causes of battery degradation, such as electrolyte decomposition, surface area, and porosity decrease; electrode volume change; binder rupture; lithium plating; and corrosion can be modeled by using electrochemical, electrical equivalent circuit, statistical, performance, and analytical modeling methods [29]. The modeling method adopted in this study is an investigative model. It requires no rigorous mathematical equation because it is software-based. Hence, this section details the modeling of the lithium-ion battery packs and their cooling circuits.

2.1. Modeling the Battery Pack

The modeling of a lithium-ion battery ($\text{LiNi}_x\text{Mn}_y\text{Co}_z\text{O}_2$) consisting of twenty-four (24) modules was performed in the MATLAB m-file environment and the battery builder in SIMSCAPE. The lithium-ion battery is a Nissan Leaf, 2017 model, for electric vehicles [30]. The cell input parameters of the battery are presented in Table 3. The computational processes engaged in this study are presented in Figure 1.

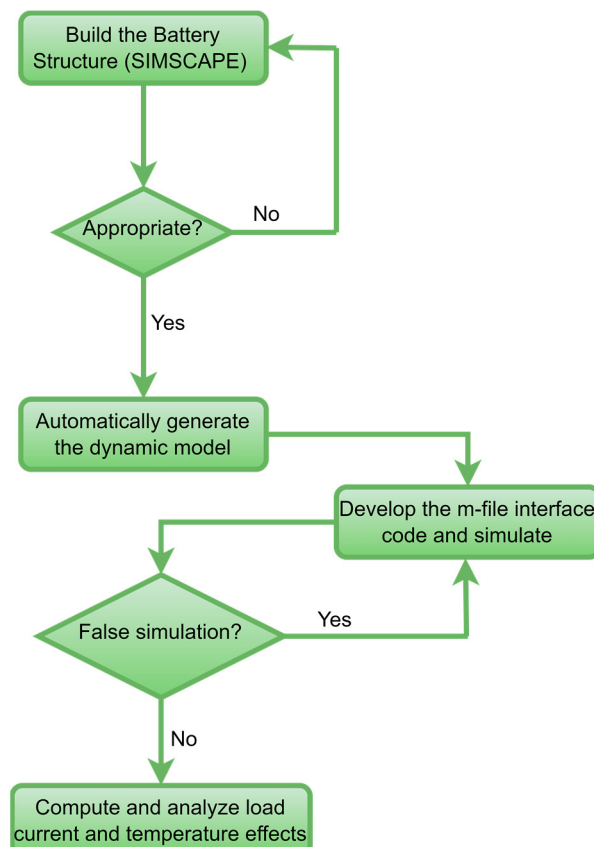


Figure 1. The computational flow chart.

Table 3. Lithium-ion cell design parameters.

Parameters	Values	Units
Height	0.216	M
Length	0.261	m
Thickness	0.007	m
Cell energy capacity	206.2	Wh
Cell mass	0.914	Kg
Cell current capacity	56.5	Ah
Cell voltage	3.65	V

Figure 2a shows the pouch geometrical structure of the cell. The battery pack modeled has a total of 192 cells, equally divided into a series connection of 96 cells. As shown in Figure 2b, the battery module assembly contains a module of 8 cells, connected in series and arranged in four (4) levels of the modules for a total assembly of twelve (12) modules. The battery pack contains two module assemblies, connected in parallel (Figure 3). Table 4 presents the specific parameters of the battery pack. All other parameters engaged in the modeling and simulation of the battery are default values from the software. Figure 4 presents the battery pack connection circuit.

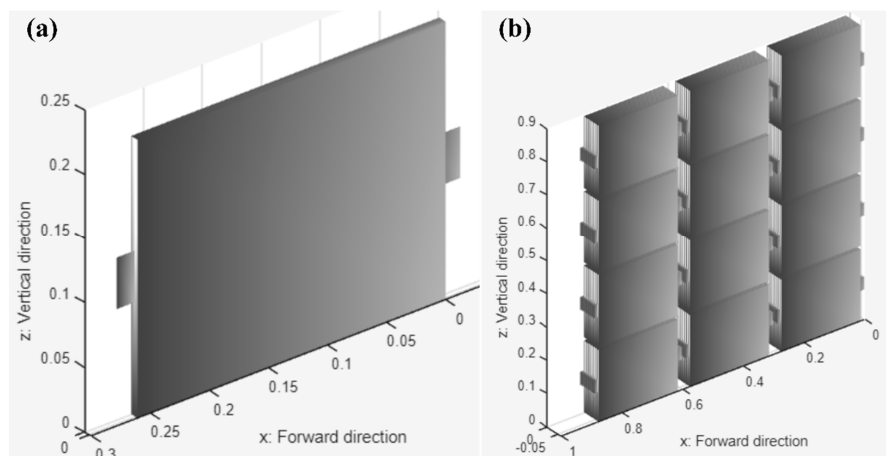
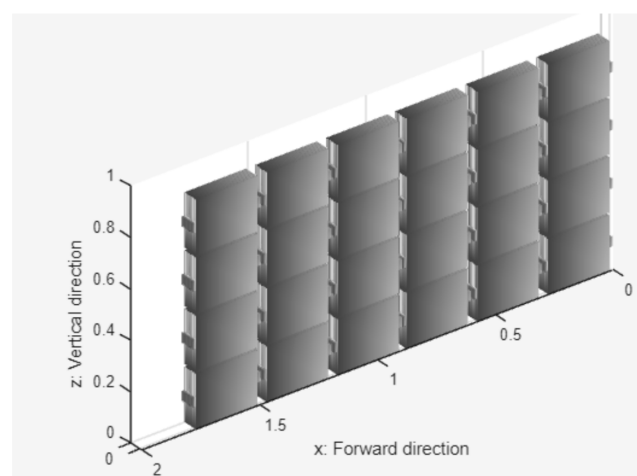
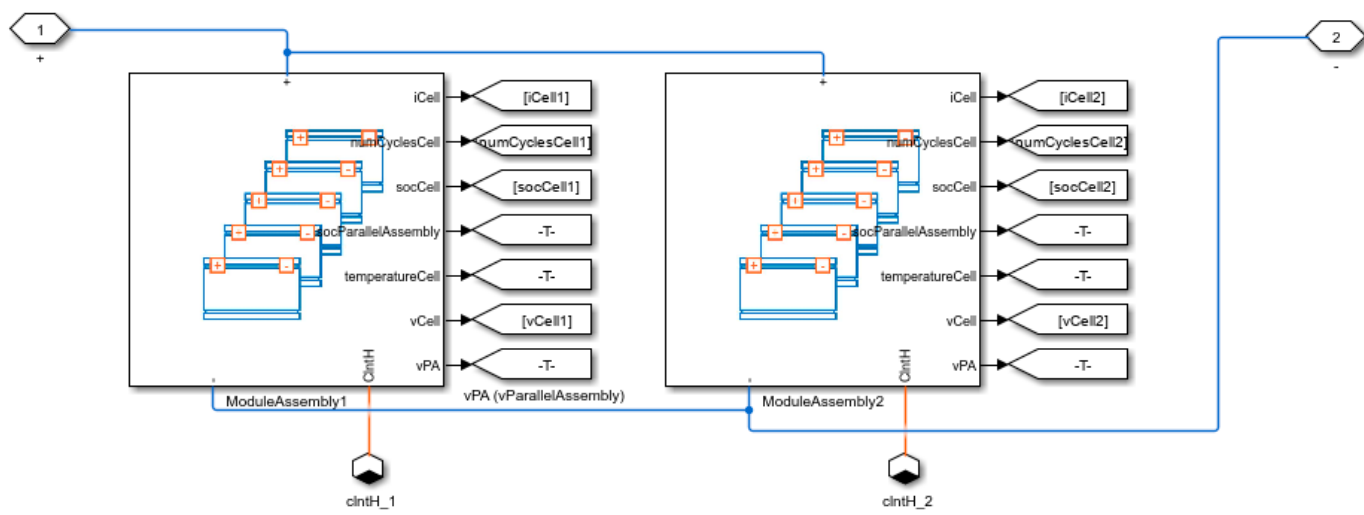
**Figure 2.** Design view of the lithium-ion (a) cell and (b) module assembly.**Figure 3.** The lithium-ion battery in a single pack (24 modules, 175.49 kg cumulative mass, 0.1131 m^3 packing volume, and 40 kWh energy capacity).

Table 4. Battery-pack-specific parameters.

Parameters	Values	Units
Current capacity	113	Ah
Voltage	350	V
Energy capacity	40	kWh
Module	8	Cells
Module assembly	12	Modules
Battery pack	2	Module assembly

**Figure 4.** The battery pack circuit connection.

2.2. Modeling the Battery with Thermal Control

The change in the condition of battery temperature may be attributed to the resistive or Joule heating, phase changes, mixing effects, electrochemical reactions, and environmental conditions [31]. Therefore, the development of cooling control systems for battery packs is essential to ensure the production of safe, efficient, and long-service-life batteries [9]. Bernardi et al. [32] developed a general balance equation for predicting or estimating battery temperature characteristics. The modification of the general balance equation by Gao et al. [33] is presented in Equation (2).

$$m \cdot c_p \cdot \frac{dT(t)}{dt} = I_{batt}^2(t) \cdot R_1 + \frac{1}{R_2} (v(t) - E(I_{batt}(t), T_{batt}(t), t) - I_{batt}(t) \cdot R_1)^2 - h_c A (T_{batt}(t) - T_a) \quad (2)$$

where m , c_p , R_1 , R_2 , E , and I_{batt} are the mass of the battery, the specific heat of the battery, resistances, battery equilibrium voltage, and battery current, respectively. Equation (2) considers the Joule heating and the heat exchange between the battery, and the environment [33]. The third and second terms of Equation (2) represent the heat exchange between the battery and the environment, while the first term is the power loss due to the resistive heating of the battery. The influence of temperature on the capacity and lifespan of the battery is a phenomenon that is central to the performance evaluation and the quantification of electric vehicles' reliability. The passivation of lithium-ion batteries, which occurs during the solid electrolyte interface formation, creates a resistance to the free diffusion of ions between the electrolyte and the electrode [34]. Of course, the increase in this resistance will lead to a decrease in the battery capacity. The continuous monitoring of the battery, in order to actively regulate its temperature to the desired range, is also important for the maintenance of the battery's capacity and lifespan [35]. This will reduce the power loss, which occurs due to the Joule heating and environmental effects.

The battery coolant control algorithm employed in this study is shown in Figure 5. The coolant system, which can be set to ON/OFF mode, operates by using the mathematical equations described in Equation (3).

$$\alpha = \begin{cases} 1, & \beta_{hot} \geq \beta_{on} \\ 0, & \beta_{hot} \leq \beta_{off} \\ \alpha_{old}, & \beta_{off} \leq \beta_{hot} \leq \beta_{on} \end{cases} \quad (3)$$

where α , α_{old} , β_{hot} , β_{on} , and β_{off} are the rate of flow temperature (this temperature is typically the difference between the ambient and coolant temperature), the previous rate of flow temperature, the temperature of the hottest cell, the switch on temperature, and switch off temperature. The rate of flow temperature equals one (1) when the coolant switch is ON to allow the passage of coolant into the battery cells, while is zero (0) when the coolant switch is OFF and there is no flow of coolant in the battery [36]. The coolant system controls the coolant flow rate. The complete battery system with the thermal control system is shown in Figure 6.

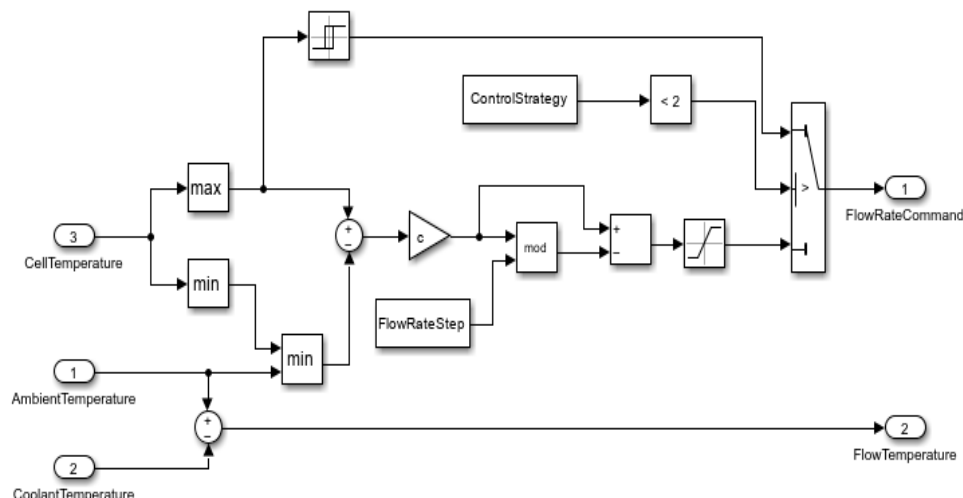


Figure 5. Battery coolant control algorithm [36].

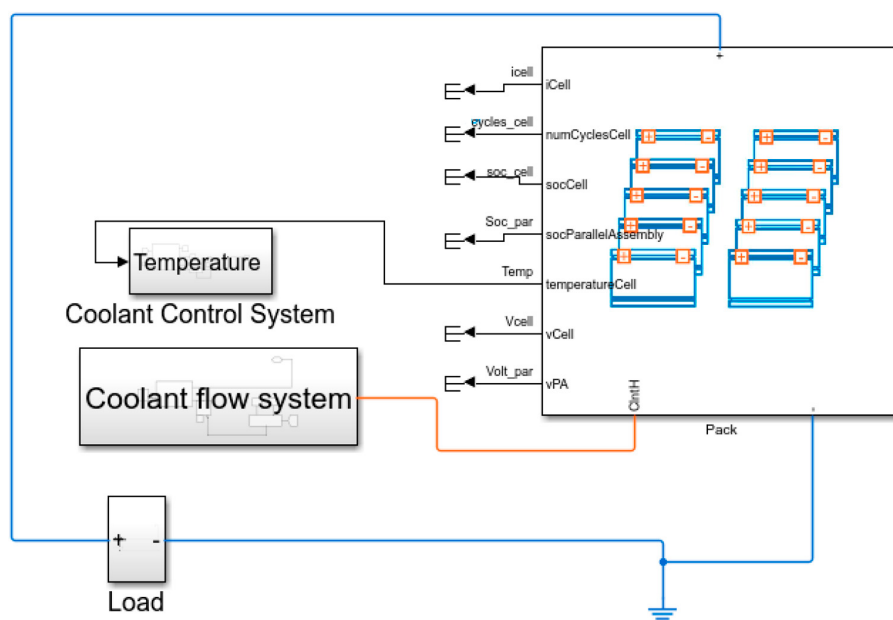


Figure 6. The lithium-ion battery, designed with a coolant control system.

3. Analytical Model

In the general Arrhenius equation, the temperature and the rate of chemical reaction have been related to describe the diffusion of chemical substances. The Arrhenius equation, shown in Equation (4), demonstrates the diffusion of ions between battery electrolytes and their electrodes.

$$C_f = Ke^{-\left(\frac{E_a}{RT}\right)} \quad (4)$$

As presented in Equation (5), Wang et al. [37] modified Equation (4) by multiplying it by the current capacity of the batteries in order to estimate the battery capacity losses.

$$C_f(\%) = Ke^{-\left(\frac{E_a}{RT_{batt}}\right)} E_c^z \quad (5)$$

where C_f , E_a , R, and T_{batt} are the battery capacity aging, activation energy, gas constant, and temperature; E_c and K are the current capacity of the battery and the pre-exponential factor, and z is the control exponent. The battery capacity loss can be formulated by relating any of the following parameters:

- Temperature and time;
- C-rate, current capacity, and temperature;
- Temperature, rate of reaction, and current capacity;
- Voltage, temperature, time, and current capacity.

In the modeling of the capacity loss of lithium-ion batteries, in terms of time, temperature, and current capacity, the expression presented in Equation (6) is as reported by Hahn et al. [26] and Ploehn et al. [38].

$$C_f(\%) \propto \sqrt{Ke^{-\left(\frac{E_a}{RT}\right)} \times t} \propto Ke^{-\left(\frac{E_a}{2RT}\right)} \sqrt{t} \propto e^{\frac{y}{T}} \sqrt{t} \quad (6)$$

y is a constant, which can be assumed; t is time in seconds.

Referring to Equation (1), the current flow in a battery is an exponential function of the temperature. Therefore, the Arrhenius equation (Equation (4)) may be more appropriate for analyzing the temperature and load current effects on battery aging. By rearranging Equation (4), Equation (7) is presented as follows:

$$C_f = Ke^{-\left(\frac{E_a}{RT}\right)} = K \left(e^{-\left(\frac{1}{T}\right)} \right)^{\frac{E_a}{R}} = K I^{\frac{E_a}{R}} = CI^b \quad (7)$$

In other words, current, I, is $e^{-\left(\frac{1}{T}\right)}$. By relating the terms in Equation (7) with the Peukert equation [39], I is the discharge current, and b is the battery constant parameter. The values of gas constant and activation energy used in this study are 31.5 kJ/mol and 8.314 J/(mol·K). The temperature ranged between 25 °C and 125 °C, and 0.5 was chosen as the battery constant parameter [37].

4. Results and Discussion

Research findings indicate that the capacity and lifespan of batteries are influenced by their operating temperature, discharge current, electrode–electrolyte interactions, and the material composition of the cathode electrode [40]. Therefore, the life of a battery is a function of its usage, its working/operating environmental condition, and the electrode materials [15,41]. Hence, the deviation in the output performances of the old battery, consisting of a thermal control system, compared to a new battery, is succinctly analyzed in this section. To simulate the temperature and voltage differences between the new and the old batteries, the battery circuits were subjected to a constant discharge time for the constant discharge currents, ranging between 30 A and 100 A, for 2 h. In addition, the end of life of the modeled batteries after 360 cycles, 1000 cycles, and 2000 cycles, as well as the performances of the modeled old battery, was compared to that of a new battery (the new and old batteries were modeled by changing their thermal resistances). The aging

of batteries generally increases as a result of the constituent resistances built up in the battery over time and repeated cycling [42]. When the transport of heat within a battery is restricted due to high thermal resistance, it can cause localized heating. This build-up of heat can lead to violent chemical reactions, such as the decomposition of the electrolyte or electrodes, which pose safety risks like thermal runaway. These reactions also degrade the battery, leading to capacity loss and accelerated aging, reducing its performance and lifespan [43].

In addition, the choice of cycles is based on the fact that lithium-ion batteries can successfully withstand discharge cycles ranging from 500 cycles to 3000 cycles if the battery is protected with a thermal management system [44–46].

4.1. Scenario 1

Generally, the differential thermal gradients in battery cells are potential threats to the safe use, cycle life, and performance of batteries. Amongst other factors, such as manufacturing errors and load imbalances, the temperature effects in battery cells operating at different cycles can lead to uneven aging of the battery cells. This effect may be a result of the non-uniform load currents, which cause the heating of the cells, and a consequential increase in power loss [47]. In addition, when battery cell temperature is non-uniformly distributed, the temperature imbalance within the battery pack can accelerate the sporadic aging of the battery [48]. In scenario 1, with all other factors set as constants, the following simulation parameters for the old battery were assumed:

- The module discharge cycle was set at 192;
- The parallel assembly discharge cycle was set at 92;
- The module thermal resistance decreased by 5% (i.e., for every 192 cycles, the thermal resistance of the module is decreased by 5%);
- The parallel assembly thermal resistance decreased by 10% (i.e., for every 92 cycles, the thermal resistance of the parallel assembly is decreased by 10%).

Shown in Figure 7 are the performance characteristics of the battery when the cooling system was disconnected from the battery and the simulation was performed for 1000 cycles. For a 30 A load current, the battery maintained a high capacity and voltage integrity, until about 1 h discharge time. Nevertheless, as the discharge time increased, the battery capacity decreased by 17%. The 40 A load current caused a capacity decrease of about 18%, while the 50 A and 100 A load currents resulted in losses of about 19% and 25%, respectively. From these results, it can be seen that the available capacity of a battery is proportional to its usage rate [49]. A battery capacity fading is generally caused by the charging and discharging cycles, loading conditions, and temperature imbalance. An increase in the discharging and charging cycles and operating temperature of the battery will result in a significant decrease in the capacity of the battery. Of course, this effect will discourage the use of electric vehicles and reduce their efficiency. It is, therefore, impractical to manufacture batteries for electric vehicles without proper thermal management control. Excessive temperature rise as a result of abnormal load can be stemmed by an appropriate thermal management system. From the report presented by Carnovale and Li [50], an electric vehicle battery's useful lifetime ends at ~75% of the battery's nominal capacity.

4.1.1. Load Current Analysis on $\text{LiNi}_x\text{Mn}_y\text{Co}_z\text{O}_2$ Battery Aging for 1000-Cycle Life

The battery coolant flow system is connected and responsible for the cooling of the old battery pack. As shown in Figure 8, when the load current on the batteries is 30 A, the voltage difference between the old and new batteries is almost negligible (i.e., 0.5%). The temperature difference is 0 °C. In addition, the coolant switching control system switches ON the coolant for the old battery at 529.5 s and at 619.5 s for the new battery. From these results, it can be inferred that the battery thermal control system can prolong the end of life of the battery. Hence, a cooling system is a significant system for the efficient utilization and operation of electric vehicle batteries [51]. The temperature, the cycling period, and

the cycling rate are phenomenon occurrences in batteries, and if not well managed, they can lead to safety problems and low performance of lithium-ion batteries. In most cases, an uncontrolled thermal effect in batteries may lead to thermal runaway. This scenario is hazardous to the users and the constituent environment. Therefore, a battery designed with a cooling control system can prevent a battery from thermal runaway [52].

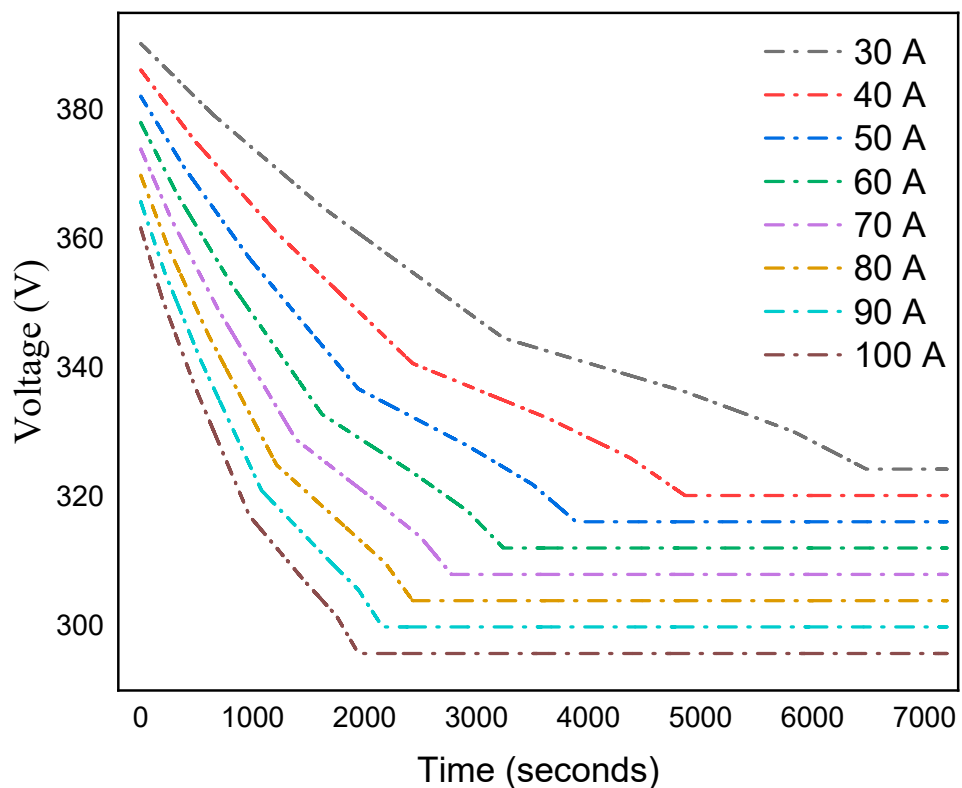


Figure 7. The effects of load currents on the battery performances without cooling.

Even though the battery modeled in this study is presumed to be thermally safe due to the incorporation of a coolant control mechanism and ideally in good health for a constant 2 h discharge time of a 30 A discharge current after 1000 cycles, as shown in Figures 8 and 9, the battery's capacity decreases as the load capacity increases. This can be explained by the fact that the energy capacity (in kWh) of the battery, with respect to its nominal voltage (V), is determined by the discharge current (A). The old lithium-ion battery shows a capacity decrease to about 74.15% after 1000 cycles when subjected to a 100 A load current for a 2 h discharge time. An important observation from the simulation results is that, at a very high load current, the degradation of the battery is less influenced by the environmental thermal change. This result agrees with the literature [53,54]. Therefore, the proper optimization of load current and thermal system response to the battery temperature differential can enhance the useful life of batteries for electric vehicles. Table 5 summarizes the voltage and coolant switching time differences between the old and new batteries.

The curves of the voltage with respect to time is an exponential two-order equation. Therefore, Equation (8) is formulated to trace the voltage profile of the battery at a given time.

$$v = c_1 e^{b_1 x} + c_2 e^{b_2 x} \quad (8)$$

where v and x are the voltage and time; c and b are constants. From the regression plot of the old battery output after 1000 cycles, Equation (9) is as presented. This equation is for a load current of 100 A.

$$v = 72e^{-0.5x} + 226e^{-0.08x} \quad (9)$$

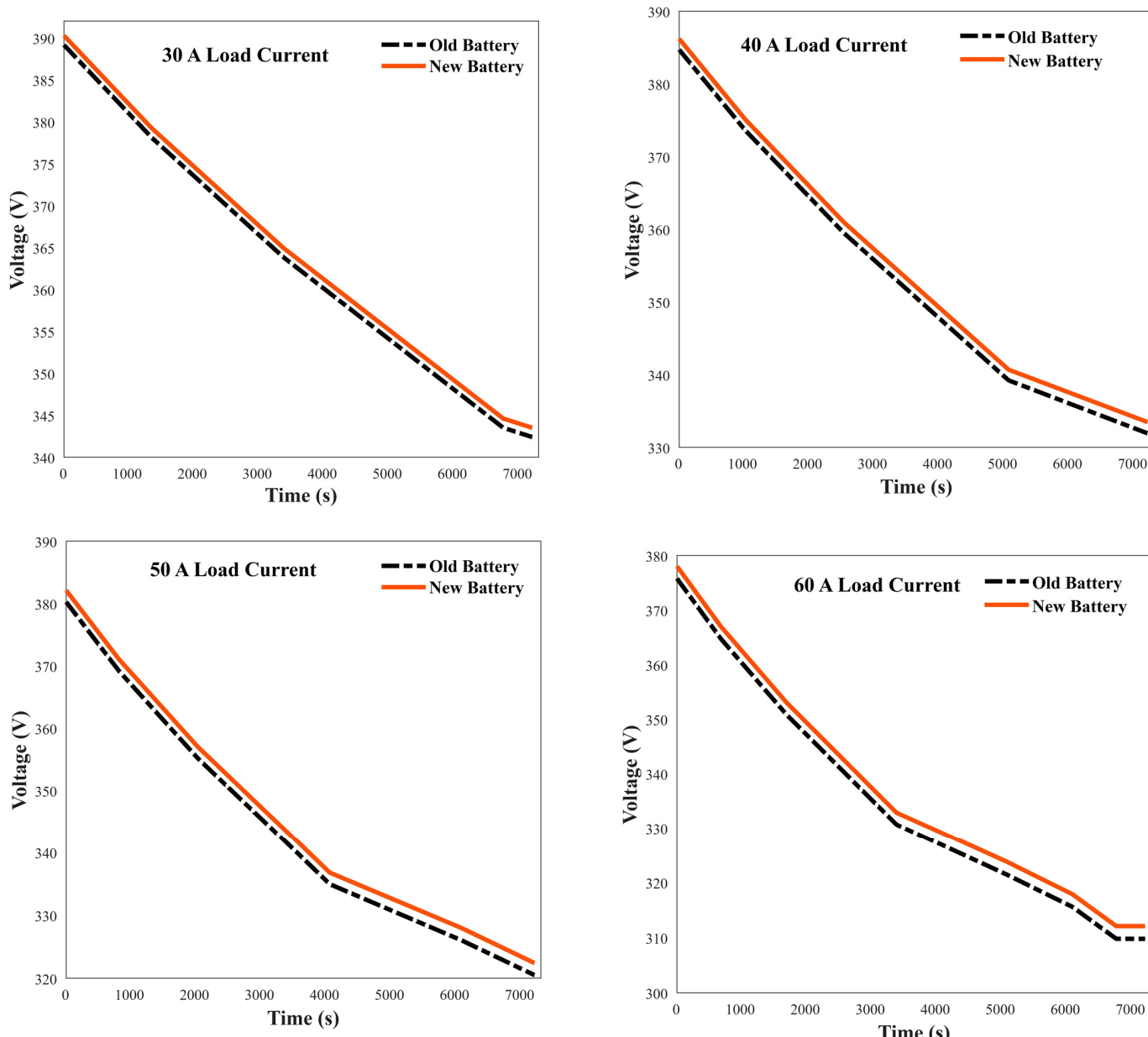


Figure 8. The aging analyses of lithium-ion batteries for load currents between 30 A and 60 A for the old and new batteries (scenario 1).

Table 5. Voltage and temperature differences between the old and new battery for 1000 cycles.

Load Current (A)	Voltage (V)	Temperature (°C)
30	2.0	0
40	2.5	1.2
50	3.1	1.9
60	3.7	2.7
70	4.41	3.7
80	4.98	4.8
90	5.58	6.1
100	6.21	7.5

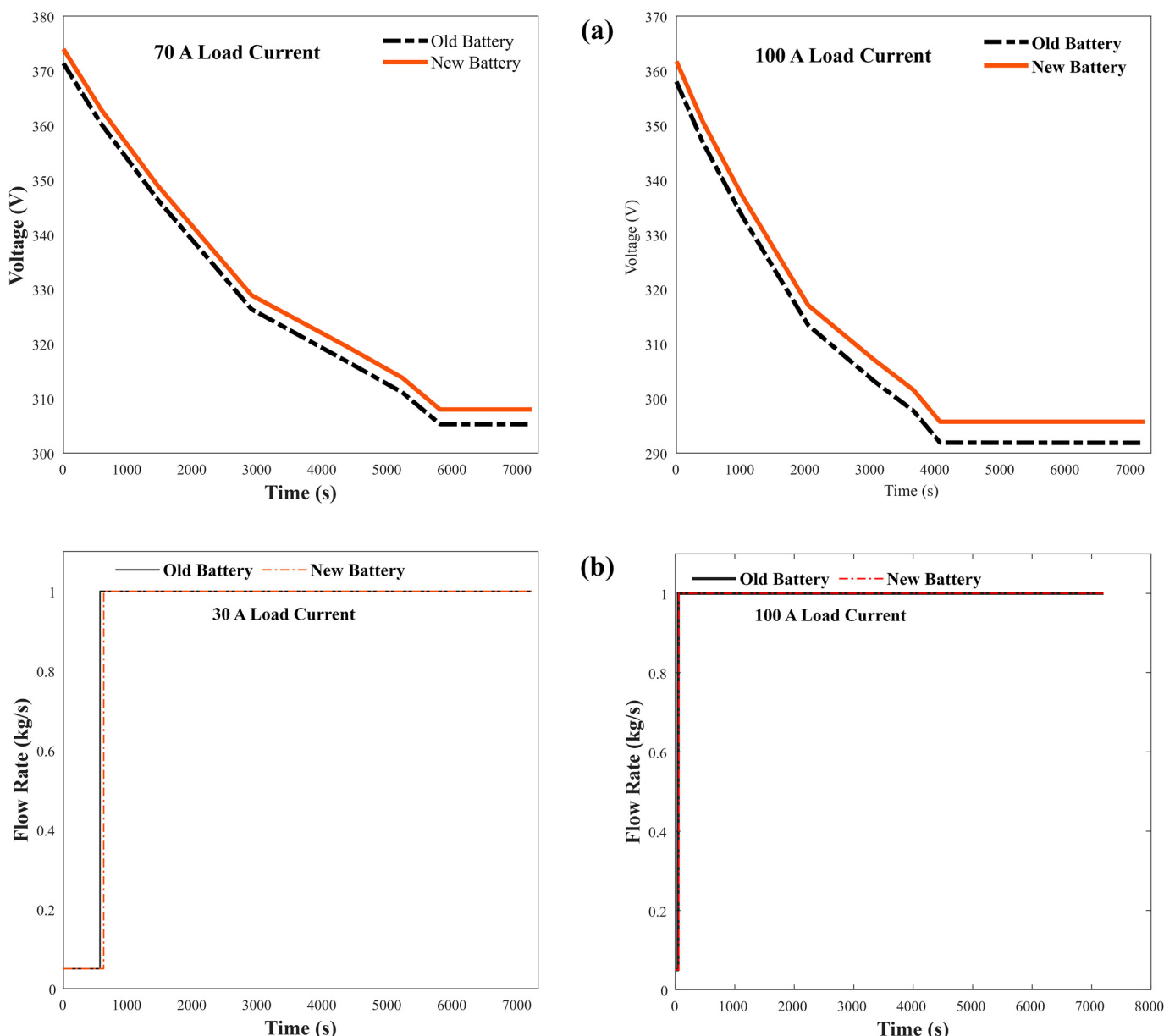


Figure 9. (a) The aging analyses of lithium-ion batteries for 70 A and 100 A load currents for old and new batteries and (b) the coolant switching hierarchy for both the old and new batteries at different load currents (scenario 1).

Figure 10 shows the power curves of the coolant switching sequence for the old and new batteries. The figure shows that the coolant switching system switches ON to cool the old battery at a faster rate than the new battery. This action is to ensure that the undesirable effect of high internal and external temperatures of the battery packs is minimized in order to improve the service life of the battery and the safety of users [55]. The heat generated by the old battery during the cycling is higher than that produced by the new battery. Hence, the importance of a battery cooling system cannot be overstated. Furthermore, in order to properly calibrate the cooling control system of the battery for an optimum/efficient operation, a simple power equation, shown in Equation (10), is proposed. This equation can be used to intelligently control and predict the switching time of the coolant system for each load.

$$y_1 = \lambda x^\delta \quad (10)$$

where y_1 and x are the discharge load current and time; λ and δ are the dependent parameter and power exponent, respectively. From the results of the regression plot of the load current and time curve of the old battery, Equation (11) is as presented. Obviously, the load current of the battery is inversely proportional to the square root of the discharge time. This observation agrees with the literature [56].

$$y_1 = 650x^{-0.5} \quad (11)$$

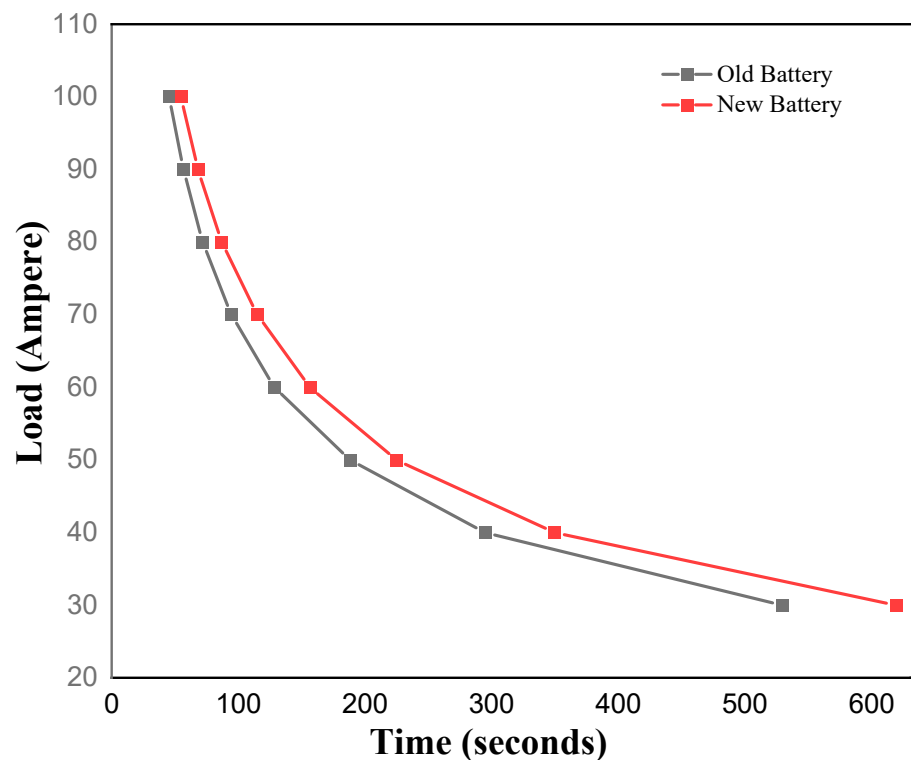


Figure 10. Coolant switching time for old and new batteries (1000-cycle life).

4.1.2. Load Current Effects on Battery Aging for 360-Cycle Life

The depth of discharge of a battery is proportional to its cycle period. In addition to the impact of the rate of discharge on the battery's capacity, a lithium-ion battery's excessive charging current will cause extra ions to deposit on the electrode's surface to form a lithium-metal layer, a phenomenon often called, lithium plating [57]. Hence, the factors contributing to the aging of batteries are numerous. As shown in Figure 11, the lithium-ion battery is less degraded after 360 cycles, in comparison to 1000 discharge cycles. At 30 A discharge current, the battery showed a deviation of about 0.97 V between 1000 and 360 cycles. Moreover, the battery's capacity kept decreasing as the load current increased. For the load currents of 40 A, 50 A, 60 A, 70 A, 80 A, 90 A, and 100 A, the voltage deviations after the batteries operated for 360 cycles and 1000 cycles are as follows: 1 V, 1.2 V, 1.81 V, 1.98 V, 2.22 V, and 2.49 V. Table 6 shows that after 360 cycles, for the 100 A discharge current, the old battery is 4.5 °C thermally deviated from the new battery. However, the thermal deviation of the battery for the same condition after 1000 cycles was 7.5 °C. Furthermore, the coolant control system was less stressful in its switching sequences when the battery was subjected to 360 cycles (Figure 12). The formulated model presented in Equation (5) can be used to predict the switching time of the battery at any cycle.

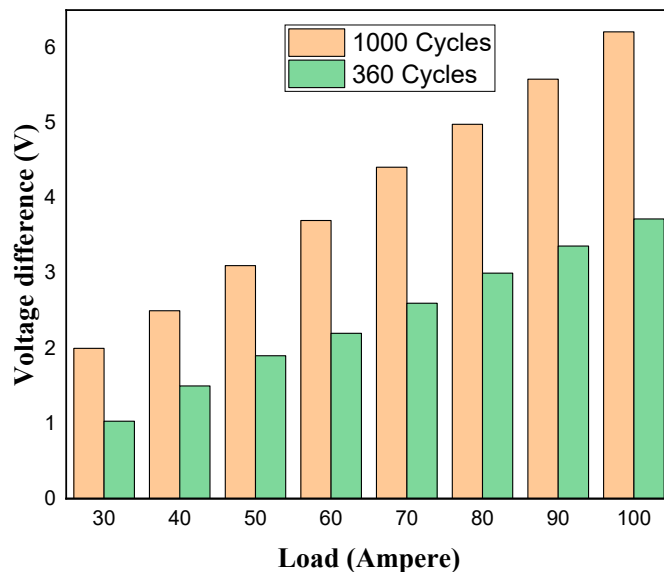


Figure 11. Performance comparison of the battery at 1000 cycles and 360 cycles (scenario 1).

Table 6. Voltage and temperature differences between the old and new batteries for 360 cycles (scenario 1).

Load Current (A)	Voltage (V)	Temperature (°C)
30	1.03	0
40	1.5	0.7
50	1.9	1.1
60	2.2	1.6
70	2.6	2.2
80	3	2.9
90	3.36	3.6
100	3.72	4.5

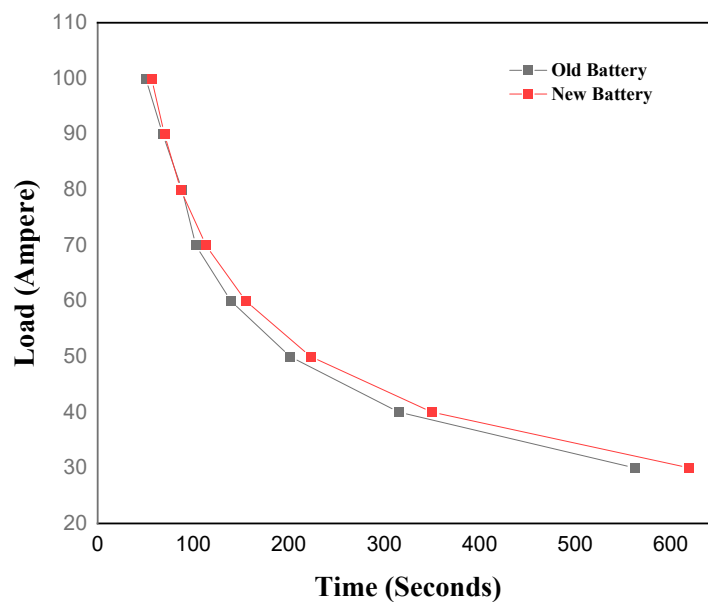


Figure 12. Coolant switching time for old and new batteries (360-cycle life).

4.2. Scenario 2

A battery pack is a multicell battery that consists of modules and modules assemblies, connected either in series or parallel. To avoid high power loss in batteries, it is essential to ensure that the discharge cycles on the modules and parallel-assembling cells are uniform and consistent. When cells are uniformly discharged, the efficiency, durability, and thermal management of the batteries can be enhanced. Therefore, in scenario 2, the following simulation parameters for the old battery were assumed:

- The module discharge cycle was set at 120;
- The parallel assembly discharge cycle was set at 120;
- The module thermal resistance decreased by 4% (i.e., for every 120 cycles, the thermal resistance of the module is decreased by 4%);
- The parallel assembly thermal resistance decreased by 4% (i.e., for every 120 cycles, the thermal resistance of the parallel assembly is decreased by 4%);
- The coolant system is connected. The purpose of the coolant system is to enhance the thermal resistance of the old battery.

Tables 7–9 provide the voltage and temperature differences between the old and the new batteries. The old and new batteries experienced capacity losses as the load current increased for all the cycles (360, 1000, and 2000). The new battery showed 88%, 78.9%, and 75.8% degradation levels when subjected to 30 A, 70 A, and 100 A load currents, respectively, for all the cycles. Moreover, the results showed less significant differences between the old and new battery capacities. This is an obvious indication that proper thermal management and uniform cell discharge cycles are appropriate measures needed to ensure sustainable usage of lithium-ion batteries in electric vehicles. The old battery showed 87.70%, 78.09%, and 74.61% degradation levels for 30 A, 70 A, and 100 A load currents, respectively, after 2000 cycles. In addition, the old battery was degraded to 87.80%, 78.38%, and 74.94% after 1000 cycles for 30 A, 70 A, and 100 A load currents. The lowest degradation, which was 75.30% for the 100 A load current, was recorded after 360 cycles. These results further confirm the fact that the accumulation of discharge cycles in batteries is a significant factor that contributes to the rapid end of life of batteries [58].

Furthermore, Figures 13–15 show the benefits of coolant systems in maximizing the useful lifetime of lithium-ion batteries. The old battery pack produced more heat than the new battery. This is due to the heating of the cells at low heat dissipation. However, the quick response of the coolant system to the rescue of the battery pack from overheating reduces the energy loss in the battery. Therefore, the voltage difference between the old and new battery packs is negligibly small. Nevertheless, the impact of load current on the degradation of the batteries is significant. Properly designed batteries with thermal management offer significant advantages in cost, safety, durability, and high-efficiency advantages [59].

Table 7. Voltage and temperature differences between the old and new batteries after 360 cycles (scenario 2).

Load Current (A)	Voltage (V)	Temperature (°C)
30	0.6	0
40	0.8	0.4
50	0.9	0.6
60	1.1	0.8
70	1.3	1.1
80	1.5	1.5
90	1.7	1.8
100	1.9	2.3

Table 8. Voltage and temperature differences between the old and new batteries after 1000 cycles (scenario 2).

Load Current (A)	Voltage (V)	Temperature (°C)
30	1.0	0
40	1.3	0.6
50	1.6	1.0
60	1.9	1.4
70	2.1	1.9
80	2.5	2.4
90	2.8	3.1
100	3.1	3.8

Table 9. Voltage and temperature differences between the old and new batteries after 2000 cycles (scenario 2).

Load Current (A)	Voltage (V)	Temperature (°C)
30	1.4	0
40	1.8	0.8
50	2.2	1.3
60	2.6	1.9
70	3.1	2.6
80	3.6	3.4
90	4.0	4.3
100	4.0	5.3

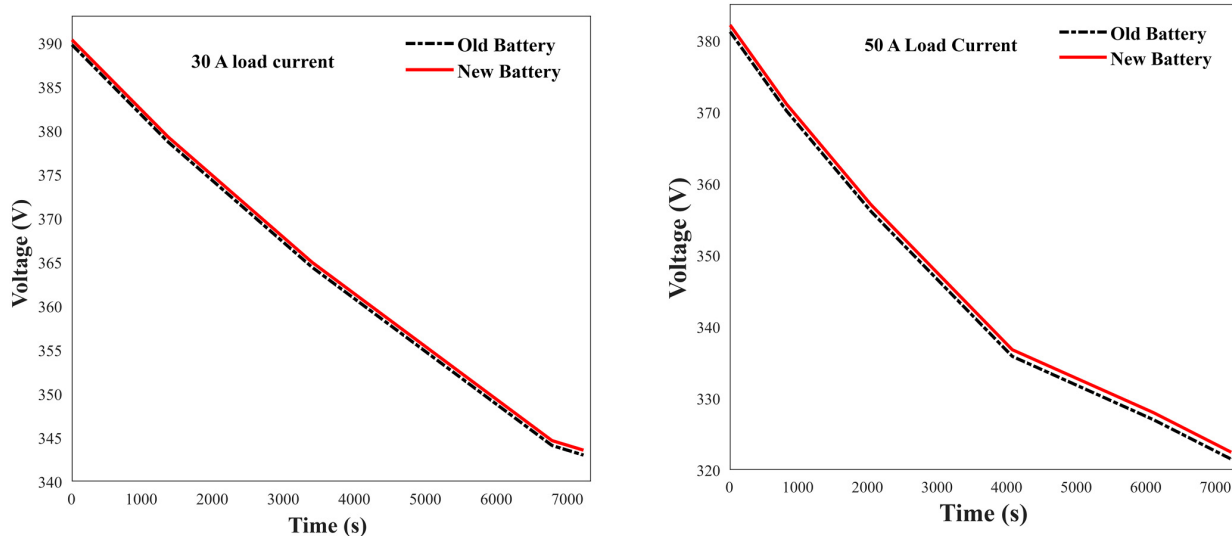


Figure 13. Cont.

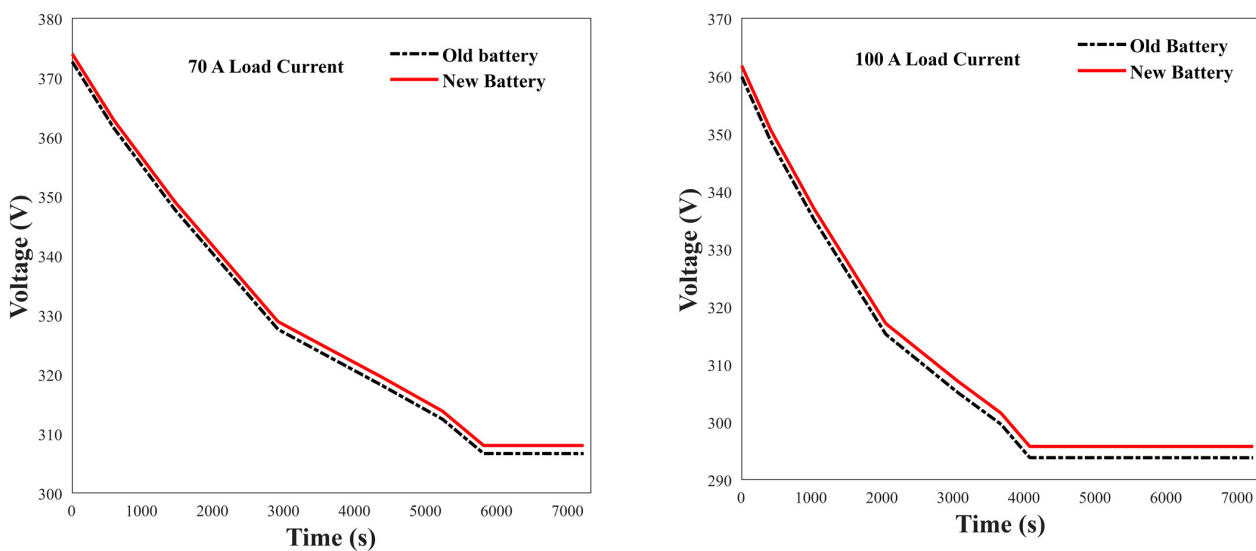


Figure 13. Voltage evolution for 360 cycles and the aging analysis of lithium-ion batteries for the 30 A, 50 A, 70 A, and 100 A load currents for old and new batteries (scenario 2).

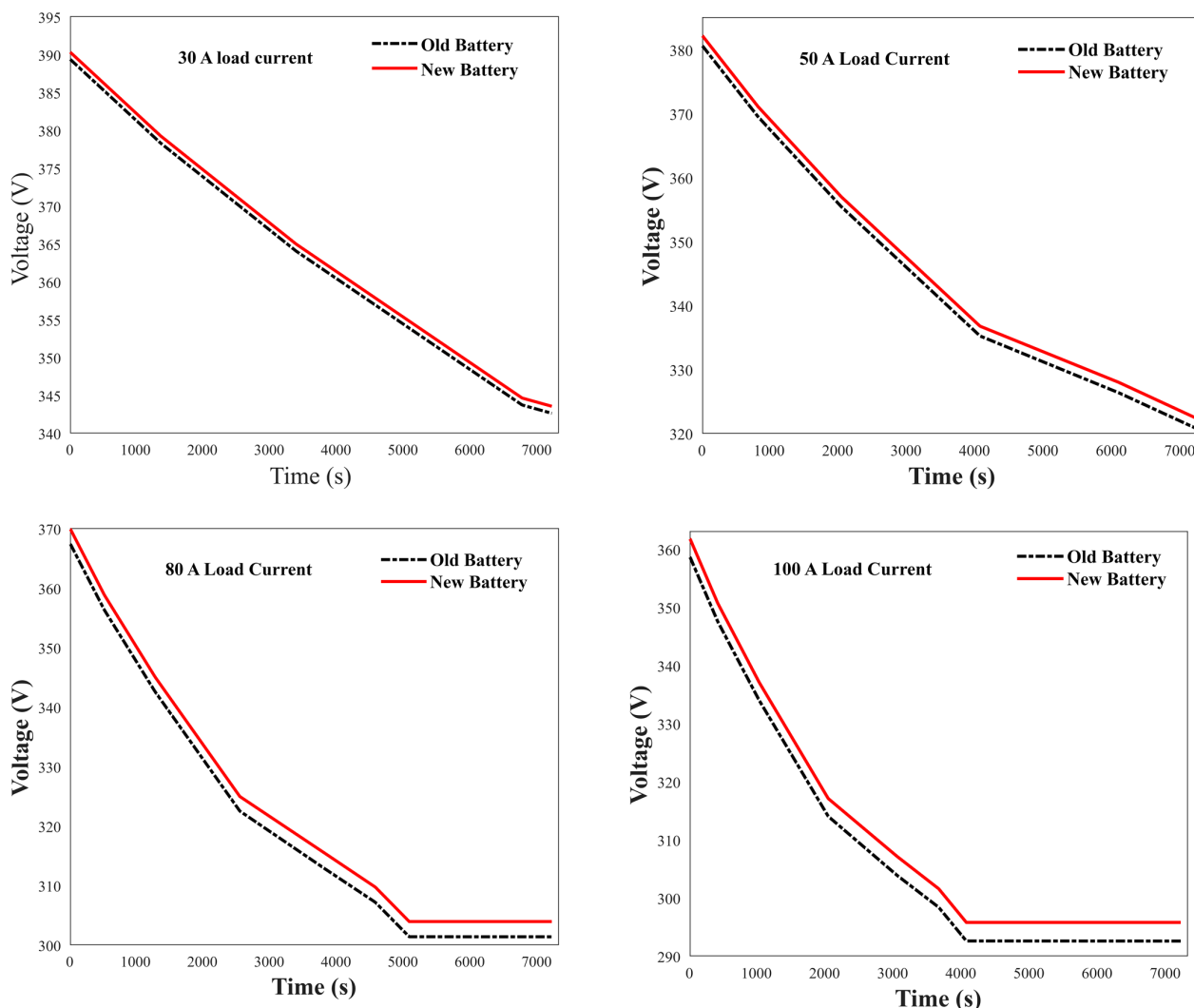


Figure 14. Voltage evolution for 1000 cycles and the aging analysis of lithium-ion batteries for the 30 A, 50 A, 80 A, and 100 A load currents for old and new batteries (scenario 2).

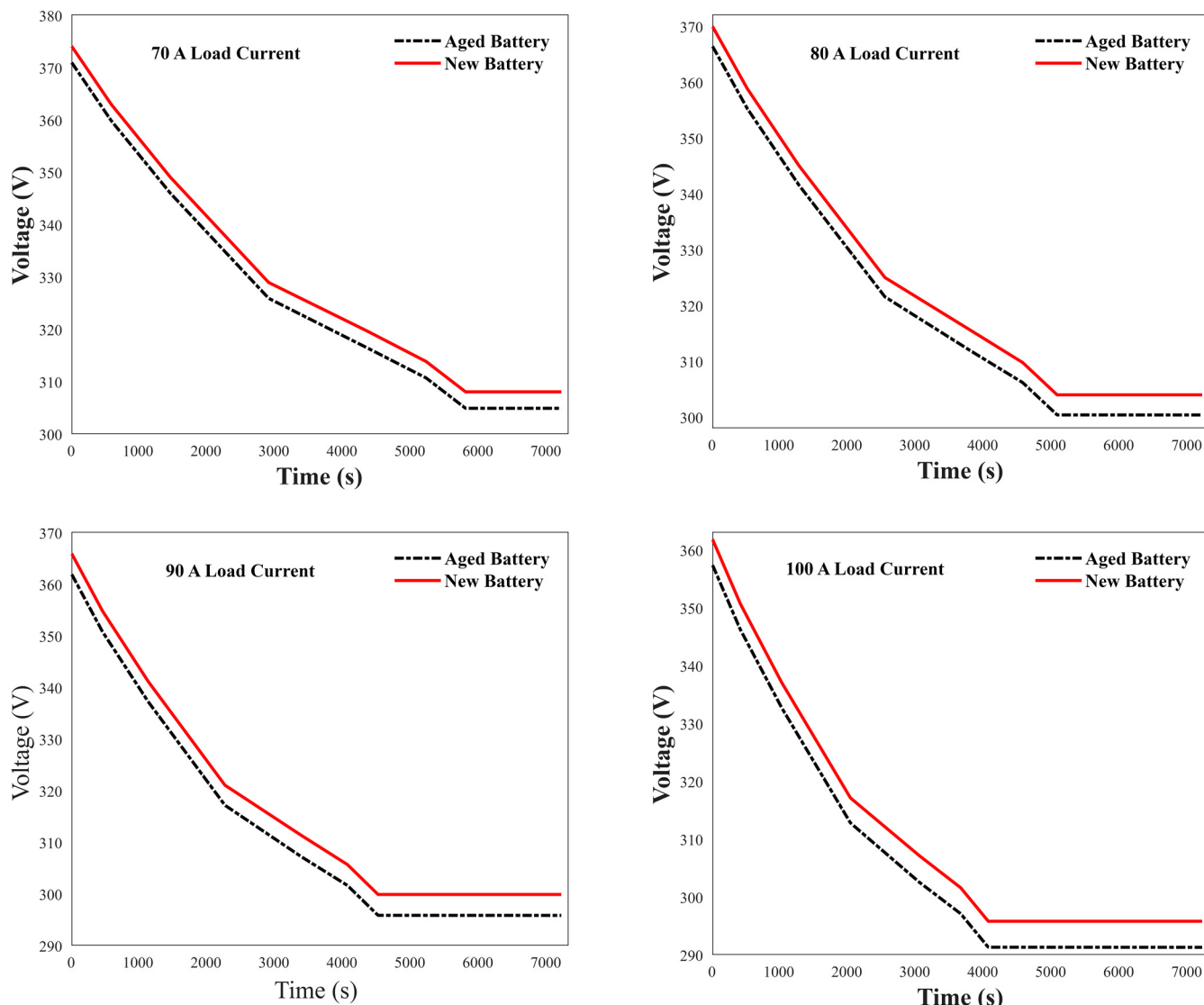


Figure 15. Voltage evolution for 2000 cycles and the aging analysis of lithium-ion batteries for the 70 A, 80 A, 90 A, and 100 A load currents for old and new batteries (scenario 2).

Lithium-ion battery temperatures must be maintained within the range of between 15 °C and 35 °C. As reported by Chavan et al. [60], a rise in the temperature of batteries by 5 °C can lead to a degradation of the battery capacities by ~2%. It is pertinent to optimize the operating temperature of batteries through optimization of the load capacity for the improvement of their performance and long lifespan. High operating temperature increases the chance of imminent self-discharge due to the loss of active materials, electrolyte contaminations, or, in general, the dissolution of the surface species of the electrolyte [61].

4.3. Recommended Cooling System

Air and liquid cooling methods have been proposed as suitable methods for lithium-ion battery thermal management [62]. Carbon allotropes, such as multiwalled carbon nanotubes, have been used to prepare nanofluid for the cooling of lithium-ion batteries [63]. Conversely, Xu et al. [61] reported that the conventional air cooling method has the disadvantage of poor thermal conductivity and that it cannot meet the requirements of high-energy-density battery systems. Therefore, a liquid-cooling system is suggested for battery thermal management, owing to its excellent efficiency and thermal conductivity [64]. Another cooling technique is the phase change process method [65]. This method has the

advantages of low cost and facile control. However, phase change materials have poor thermal conductivity [66]. Therefore, the liquid flow cooling system employed in this study is appropriate, and it is recommended for the practical thermal management of lithium-ion batteries. The study conducted by Sadeh et al. [67] showed that a flow cooling system has the advantage of reducing the inhomogeneity of temperature distribution in battery packs. In future, gel-cooling, e.g., polymer hydrogels with adequate conductivity, can also be considered.

4.4. Further Discussion and Validation

As shown in Figure 16, the effect of temperature and current on the battery capacity is demonstrated by the model presented in Equation (7). From the figure, it can be suggested that the battery operating temperature should be kept as low as 25 °C. The tendency for the solid electrolyte interface to increase abounds during battery cycling. The thickness of the solid electrolyte interface has a direct incremental impact on heat generation. Therefore, battery pack capacity can be easily degraded when operated at a high temperature, coupled with large solid electrolyte interface thickness [68]. Battery capacity loss also increases due to the structural deformation of the battery electrodes. The defect in the electrodes can lead to the cracking and fracturing of the electrodes. In summary, the electrode volume expansion, leading to cracks during cycling, the lithium loss as a result of solid electrolyte interface thickness, and the reformation of solid electrolyte interface on the electrode crack surface are agents of battery capacity loss [69]. These factors are usually influenced by the cycle time, temperature, and current loadings.

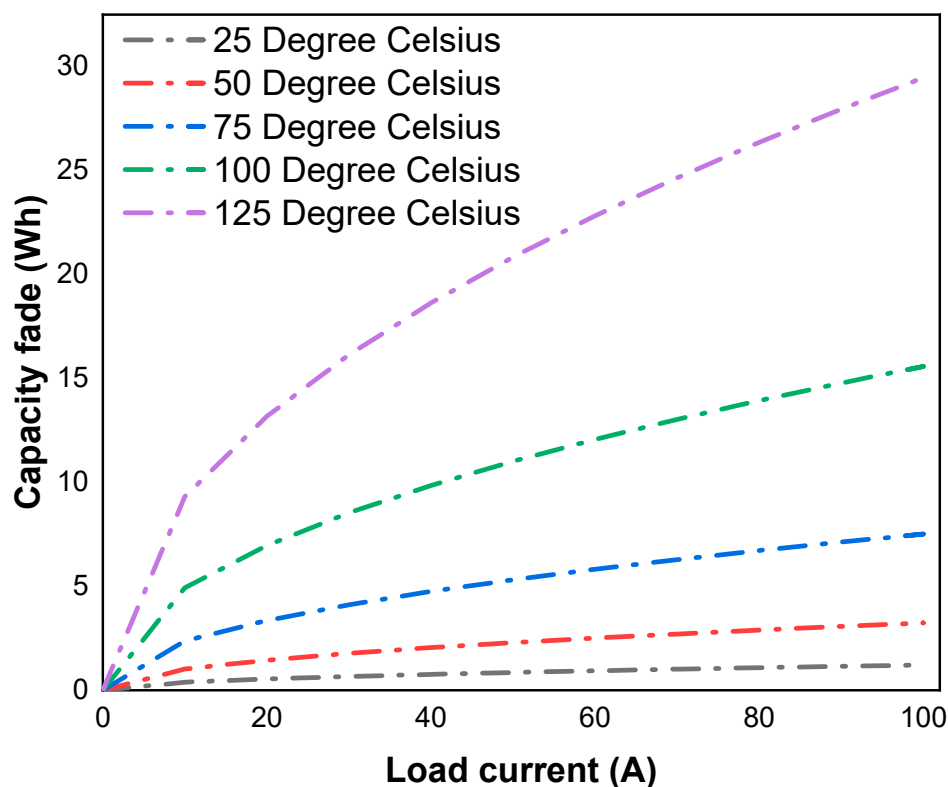


Figure 16. Temperature and load current effects on battery capacity.

To evaluate the robustness of the investigative model engaged in this study, the results of the model were compared with the available experimental data [70]. Specifically, as previously discussed, it was observed from the experimental data that the battery exhibited a reduced capacity and low-rate performance as the load current increased from 2 A to 5 A (Figure 17a,b). It is important to note that, while retaining the original information of the experimental data, scaling was applied in order to obtain a balanced and correlated

comparison between the experimental and model results. The simulated battery, after 360 discharge cycles, for 30 A and 50 A current load conditions, was compared with the experimental data. As illustrated in Figure 17, the model produces results that closely agree with experimental data, demonstrating a high level of accuracy. The model's prediction showed an average deviation of ~2.16% from the experimental data. This result indicates robust performance in the simulation of the batteries under varying load conditions.

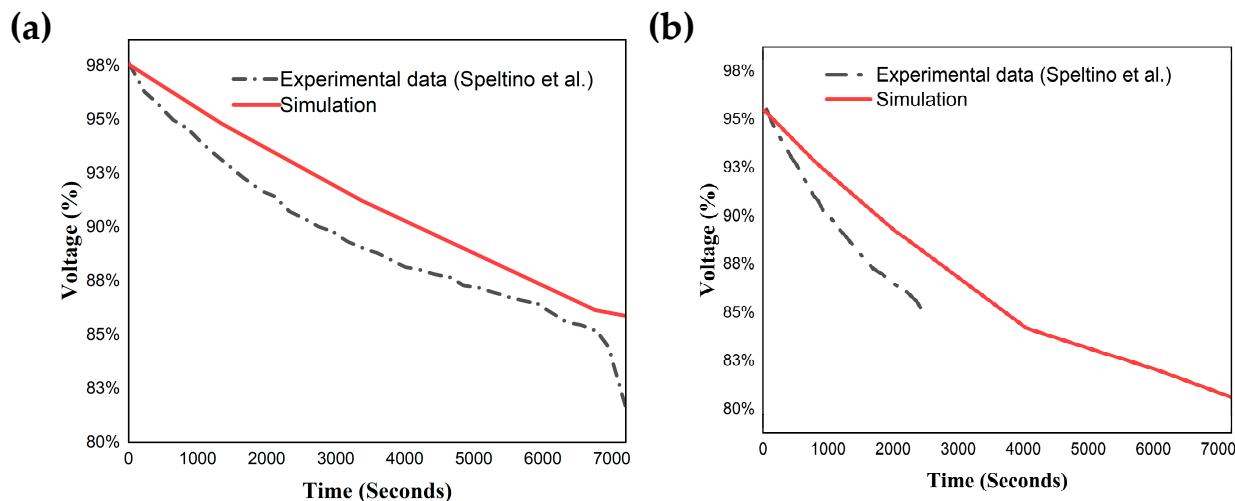


Figure 17. Comparison of model results with experimental data for (a) 2 A and (b) 5 A load current conditions. The experimental data were scaled to achieve a balanced comparison and correlation between the experimental and model results [70].

Moreover, the results obtained in this study agree with the literature. For instance, Ouyang et al. [71] observed that the load current on batteries has direct consequential effects on the battery end of life. A high current rate causes a potential reduction in the capacity of batteries and their performances due to the violent internal electrochemical reactions within the battery. Therefore, the continuous operation of a battery at a high current rate can lead to quick degradation of the battery. A finding from the report presented by Zhang et al. [72] revealed that high load current increases the internal heat generated by the batteries. The period the load current is sustained on the battery determines the rate at which the battery degrades. Furthermore, the investigation conducted by Baek et al. [73] on lithium-ion batteries, also corroborated the effect of discharge cycles on the battery capacity reduction. As the discharge cycle increased, the capacity reduction of the lithium-ion batteries increased. The comparison of the experimental and simulation study carried out by Carnovale and Li [50] also displayed the capacity degradation of a battery as the discharge cycles increased.

5. Conclusions

Herein, this study presents the effects of load current on the capacity performances of lithium-ion batteries. The significance of a coolant system in lithium-ion batteries was discussed by comparing two different batteries. The investigative model developed in this study is efficient in evaluating thermal performances and the end of life of the batteries studied for electric vehicles. It is apparent that the thickness of the solid electrolyte interface and the cracking and fracturing of an electrode, which contribute to the battery aging and capacity loss, result from thermal instability, cycling, and excessive loadings of the battery. Hence, the incorporation of effective cooling systems in electric vehicle batteries and the rigid optimization of their load current are an important approach to reducing the aging and capacity loss of batteries. In this study, the lithium-ion battery was designed with a cell current capacity of 56.5 Ah, a cell energy capacity of 206.2 Wh, and 192 total cells, which were equally divided into a series connection of 96 cells. From the findings of this study, for

scenario 1, when the battery was simulated without a cooling system and after 1000 cycles, the following results were observed:

- For a 30 A load current, the battery maintained a high capacity and voltage integrity until about 1 h. However, as the discharge time increased, the battery capacity decreased by 17%.
- The 40 A load current caused a capacity decrease of about 18%, while the 50 A and 100 A load currents resulted in losses of about 19% and 25%, respectively.

Furthermore, when the cooling system was incorporated into the battery, the thermal deviation of the old battery from the new battery, cycled for 360 cycles and 1000 cycles at a 100 A load current, was 4.5 °C and 7.5 °C, respectively. The lithium-ion battery showed a capacity decrease to about 74.15% after 1000 cycles for a load current of 100 A. In addition, for scenario 2, the old battery showed 87.70%, 78.09%, and 74.61% degradation levels for the 30 A, 70 A, and 100 A load currents after 2000 cycles. After 1000 cycles, the degradation levels were 87.80%, 78.38%, and 74.94% for 30 A, 70 A, and 100 A load currents, while the lowest degradation level, which was 75.30% for the 100 A load current, was recorded after 360 cycles. Based on the results obtained in this study, equations were developed to enhance calibration accuracy and to model essential characteristics of batteries, such as voltage behavior and cooling switch time.

It can be concluded from the obtained results that the capacity loss in electric vehicle batteries increased as the load current and temperature increased. However, the significance of temperature was less pronounced when the battery was exposed to excessive load current. This underscores the need for electric vehicle battery designers to focus not only on thermal regulation, but also on mitigating the effects of high-load currents. Addressing both aspects will help to maintain the battery's longevity and performance across a wider range of operating conditions. Therefore, lithium-ion batteries for electric vehicles must be fabricated with appropriate cooling systems, low-energy-consuming electric motors, and devices.

Author Contributions: Conceptualization, O.F.; methodology, O.F.; software, O.F.; validation, R.S.; formal analysis, O.F.; investigation, O.F.; writing—original draft preparation, O.F.; writing—review and editing, R.S.; visualization, O.F.; supervision, Y.H., R.S. and W.K. All authors have read and agreed to the published version of the manuscript.

Funding: This research received no external funding.

Data Availability Statement: The original contributions presented in the study are included in the article, further inquiries can be directed to the corresponding author.

Acknowledgments: Appreciation and many thanks to the Tshwane University of Technology, South Africa, for the financial support.

Conflicts of Interest: The authors declare no conflicts of interest.

Nomenclature

I_{batt}	Battery current
T_{batt}	Battery temperature
m	Mass of the battery
c_p	Specific heat capacity of the battery
R	Resistance
E	Equilibrium voltage
v	Battery voltage
T_a	Ambient temperature
A	Surface area
h_c	Heat transfer coefficient
α	Rate of flow temperature
α_{old}	Initial rate of flow temperature

β_{hot}	Temperature of the hottest cell
β_{on} and β_{off}	Switch on and switch off temperatures
C_f	Battery capacity aging
E_a	Activation energy
R	Gas constant
T	Temperature
E_c	Current capacity of the battery
K	Pre-exponential factor
z	Control exponent
y, b, c	Constants
I	Discharge current
t, x	Time
y_1	Discharge load current
λ and δ	Dependent parameter and power exponent

References

- Zhao, J.; Xi, X.; Na, Q.; Wang, S.; Kadry, S.N.; Kumar, P.M. The technological innovation of hybrid and plug-in electric vehicles for environment carbon pollution control. *Environ. Impact Assess. Rev.* **2021**, *86*, 106506. [[CrossRef](#)]
- Folorunso, O.; Sadiku, R.; Hamam, Y. Dispatchable generation analysis and prediction by using machine learning: A case study of South Africa. *e-Prime-Adv. Electr. Eng. Electron. Energy* **2024**, *9*, 100701. [[CrossRef](#)]
- Märtz, A.; Plötz, P.; Jochem, P. Global perspective on CO₂ emissions of electric vehicles. *Environ. Res. Lett.* **2021**, *16*, 054043. [[CrossRef](#)]
- Tie, S.F.; Tan, C.W. A review of energy sources and energy management system in electric vehicles. *Renew. Sustain. Energy Rev.* **2013**, *20*, 82–102. [[CrossRef](#)]
- Folorunso, O.; Hamam, Y.; Sadiku, R.; Ray, S.S.; Adekoya, G.J. Investigation of graphene loaded polypyrrole for lithium-ion battery. *Mater. Today Proc.* **2021**, *38*, 635–638. [[CrossRef](#)]
- Folorunso, O.; Hamam, Y.; Sadiku, R.; Ray, S.S.; Adekoya, G.J. Theoretical analysis of borophene for lithium ion electrode. *Mater. Today Proc.* **2021**, *38*, 485–489. [[CrossRef](#)]
- Gao, Y.; Pan, Z.; Sun, J.; Liu, Z.; Wang, J. High-energy batteries: Beyond lithium-ion and their long road to commercialisation. *Nano-Micro Lett.* **2022**, *14*, 94. [[CrossRef](#)]
- Langdon, J.; Manthiram, A. A perspective on single-crystal layered oxide cathodes for lithium-ion batteries. *Energy Storage Mater.* **2021**, *37*, 143–160. [[CrossRef](#)]
- Chen, D.; Jiang, J.; Kim, G.-H.; Yang, C.; Pesaran, A. Comparison of different cooling methods for lithium ion battery cells. *Appl. Therm. Eng.* **2016**, *94*, 846–854. [[CrossRef](#)]
- Saw, L.; Somasundaram, K.; Ye, Y.; Tay, A. Electro-thermal analysis of Lithium Iron Phosphate battery for electric vehicles. *J. Power Sources* **2014**, *249*, 231–238. [[CrossRef](#)]
- Moayedi, H. Performance improvement and thermal management of a lithium-ion battery by optimizing tab locations and cell aspect ratio. *Int. J. Heat Mass Transf.* **2023**, *214*, 124456. [[CrossRef](#)]
- Ma, S.; Jiang, M.; Tao, P.; Song, C.; Wu, J.; Wang, J.; Deng, T.; Shang, W. Temperature effect and thermal impact in lithium-ion batteries: A review. *Prog. Nat. Sci. Mater. Int.* **2018**, *28*, 653–666. [[CrossRef](#)]
- Jiang, Z.; Qu, Z.; Wang, Q. Experimental and numerical investigation of fast preheating of lithium ion pouch cell via low-power inductive heating in cold climate. *Int. J. Heat Mass Transf.* **2023**, *214*, 124381. [[CrossRef](#)]
- Hamut, H.; Dincer, I.; Naterer, G. Performance assessment of thermal management systems for electric and hybrid electric vehicles. *Int. J. Energy Res.* **2013**, *37*, 1–12. [[CrossRef](#)]
- Palacín, M.R.; de Guibert, A. Why do batteries fail? *Science* **2016**, *351*, 1253292. [[CrossRef](#)]
- Paarmann, S.; Cloos, L.; Technau, J.; Wetzel, T. Measurement of the Temperature Influence on the Current Distribution in Lithium-Ion Batteries. *Energy Technol.* **2021**, *9*, 2000862. [[CrossRef](#)]
- Vermeer, W.; Mouli, G.R.C.; Bauer, P. A comprehensive review on the characteristics and modeling of lithium-ion battery aging. *IEEE Trans. Transp. Electrif.* **2021**, *8*, 2205–2232. [[CrossRef](#)]
- Rahman, T.; Alharbi, T. Exploring Lithium-Ion Battery Degradation: A Concise Review of Critical Factors, Impacts, Data-Driven Degradation Estimation Techniques, and Sustainable Directions for Energy Storage Systems. *Batteries* **2024**, *10*, 220. [[CrossRef](#)]
- Ahmad, Z.; Venturi, V.; Hafiz, H.; Viswanathan, V. Interfaces in solid electrolyte interphase: Implications for lithium-ion batteries. *J. Phys. Chem. C* **2021**, *125*, 11301–11309. [[CrossRef](#)]
- An, S.J.; Li, J.; Daniel, C.; Mohanty, D.; Nagpure, S.; Wood III, D.L. The state of understanding of the lithium-ion-battery graphite solid electrolyte interphase (SEI) and its relationship to formation cycling. *Carbon* **2016**, *105*, 52–76. [[CrossRef](#)]
- Petzl, M.; Kasper, M.; Danzer, M.A. Lithium plating in a commercial lithium-ion battery—A low-temperature aging study. *J. Power Sources* **2015**, *275*, 799–807. [[CrossRef](#)]
- Edge, J.S.; O’Kane, S.; Prosser, R.; Kirkaldy, N.D.; Patel, A.N.; Hales, A.; Ghosh, A.; Ai, W.; Chen, J.; Yang, J. Lithium ion battery degradation: What you need to know. *Phys. Chem. Chem. Phys.* **2021**, *23*, 8200–8221. [[CrossRef](#)] [[PubMed](#)]

23. Jalilantabar, F.; Mamat, R.; Kumarasamy, S. Prediction of lithium-ion battery temperature in different operating conditions equipped with passive battery thermal management system by artificial neural networks. *Mater. Today Proc.* **2022**, *48*, 1796–1804. [[CrossRef](#)]
24. Wimarshana, B.; Bin-Mat-Arishad, I.; Fly, A. Parameter sensitivity analysis of a physico-chemical lithium-ion battery model with combined discharge voltage and electrochemical impedance data. *J. Power Sources* **2022**, *527*, 231125. [[CrossRef](#)]
25. Li, A.; Yuen, A.C.Y.; Wang, W.; Chen, T.B.Y.; Lai, C.S.; Yang, W.; Wu, W.; Chan, Q.N.; Kook, S.; Yeoh, G.H. Integration of computational fluid dynamics and artificial neural network for optimization design of battery thermal management system. *Batteries* **2022**, *8*, 69. [[CrossRef](#)]
26. Hahn, S.L.; Storch, M.; Swaminathan, R.; Obry, B.; Bandlow, J.; Birke, K.P. Quantitative validation of calendar aging models for lithium-ion batteries. *J. Power Sources* **2018**, *400*, 402–414. [[CrossRef](#)]
27. The-MathWorks-Inc. *MATLAB Version: R2023a Update 3 (9.14.0.2286388)*; The MathWorks Inc.: Natick, MA, USA, 2023.
28. Han, X.; Lu, L.; Zheng, Y.; Feng, X.; Li, Z.; Li, J.; Ouyang, M. A review on the key issues of the lithium ion battery degradation among the whole life cycle. *ETransportation* **2019**, *1*, 100005. [[CrossRef](#)]
29. De Gennaro, M.; Paffumi, E.; Martini, G.; Giallardo, A.; Pedroso, S.; Loiselle-Lapointe, A. A case study to predict the capacity fade of the battery of electrified vehicles in real-world use conditions. *Case Stud. Transp. Policy* **2020**, *8*, 517–534. [[CrossRef](#)]
30. Calearo, L.; Thingvad, A.; Marinelli, M. Modeling of battery electric vehicles for degradation studies. In Proceedings of the 2019 54th International Universities Power Engineering Conference (UPEC), Bucharest, Romania, 3–6 September 2019; IEEE: Piscataway, NJ, USA, 2019; pp. 1–6.
31. Hu, Z.; Liu, F.; Chen, P.; Xie, C.; Huang, M.; Hu, S.; Lu, S. Experimental study on the mechanism of frequency-dependent heat in AC preheating of lithium-ion battery at low temperature. *Appl. Therm. Eng.* **2022**, *214*, 118860. [[CrossRef](#)]
32. Bernardi, D.; Pawlikowski, E.; Newman, J. A general energy balance for battery systems. *J. Electrochem. Soc.* **1985**, *132*, 5. [[CrossRef](#)]
33. Gao, L.; Liu, S.; Dougal, R.A. Dynamic lithium-ion battery model for system simulation. *IEEE Trans. Compon. Packag. Technol.* **2002**, *25*, 495–505.
34. Folorunso, O.; Olukanmi, P.O.; Shongwe, T. Progress towards sustainable energy storage: A concise review. *Eng. Rep.* **2023**, *5*, e12731. [[CrossRef](#)]
35. Wang, Q.; Jiang, B.; Li, B.; Yan, Y. A critical review of thermal management models and solutions of lithium-ion batteries for the development of pure electric vehicles. *Renew. Sustain. Energy Rev.* **2016**, *64*, 106–128. [[CrossRef](#)]
36. The-MathWorks-Inc. *Battery Coolant Control. Battery Coolant Control algorithm* Since R2022b; The MathWorks Inc.: Natick, MA, USA, 2024.
37. Wang, J.; Liu, P.; Hicks-Garner, J.; Sherman, E.; Soukiazian, S.; Verbrugge, M.; Tataria, H.; Musser, J.; Finamore, P. Cycle-life model for graphite-LiFePO₄ cells. *J. Power Sources* **2011**, *196*, 3942–3948. [[CrossRef](#)]
38. Ploehn, H.J.; Ramadas, P.; White, R.E. Solvent diffusion model for aging of lithium-ion battery cells. *J. Electrochem. Soc.* **2004**, *151*, A456. [[CrossRef](#)]
39. Doerffel, D.; Sharikh, S.A. A critical review of using the Peukert equation for determining the remaining capacity of lead-acid and lithium-ion batteries. *J. Power Sources* **2006**, *155*, 395–400. [[CrossRef](#)]
40. Zeng, L.; Hu, Y.; Lu, C.; Pan, G. Performance evaluation of lithium battery pack based on MATLAB simulation with lumped parameter thermal model. *Energy Sci. Eng.* **2023**, *11*, 2614–2629. [[CrossRef](#)]
41. Xie, J.; Zhang, Q. Recent progress in rechargeable lithium batteries with organic materials as promising electrodes. *J. Mater. Chem. A* **2016**, *4*, 7091–7106. [[CrossRef](#)]
42. Shen, W.; Wang, N.; Zhang, J.; Wang, F.; Zhang, G. Heat generation and degradation mechanism of lithium-ion batteries during high-temperature aging. *ACS Omega* **2022**, *7*, 44733–44742. [[CrossRef](#)]
43. Lyu, P.; Liu, X.; Qu, J.; Zhao, J.; Huo, Y.; Qu, Z.; Rao, Z. Recent advances of thermal safety of lithium ion battery for energy storage. *Energy Storage Mater.* **2020**, *31*, 195–220. [[CrossRef](#)]
44. Gao, W.; Cao, Z.; Kurdkandi, N.V.; Fu, Y.; Mi, C. Evaluation of the second-life potential of the first-generation Nissan Leaf battery packs in energy storage systems. *eTransportation* **2024**, *20*, 100313. [[CrossRef](#)]
45. Gao, W.; Cao, Z.; Fu, Y.; Turchiano, C.; Kurdkandi, N.V.; Gu, J.; Mi, C. Comprehensive study of the aging knee and second-life potential of the Nissan Leaf e+ batteries. *J. Power Sources* **2024**, *613*, 234884. [[CrossRef](#)]
46. Shchurov, N.I.; Dedov, S.I.; Malozymov, B.V.; Shtang, A.A.; Martyushev, N.V.; Klyuev, R.V.; Andriashin, S.N. Degradation of lithium-ion batteries in an electric transport complex. *Environ. Monit. Assess.* **2021**, *14*, 8072. [[CrossRef](#)]
47. Baumann, M.; Wildfeuer, L.; Rohr, S.; Lienkamp, M. Parameter variations within Li-Ion battery packs—Theoretical investigations and experimental quantification. *J. Energy Storage* **2018**, *18*, 295–307. [[CrossRef](#)]
48. Saw, L.; Ye, Y.; Tay, A. Electro-thermal analysis and integration issues of lithium ion battery for electric vehicles. *Appl. Energy* **2014**, *131*, 97–107. [[CrossRef](#)]
49. Yang, X.; Chen, Y.; Li, B.; Luo, D. Battery states online estimation based on exponential decay particle swarm optimization and proportional-integral observer with a hybrid battery model. *Energy* **2020**, *191*, 116509.
50. Carnovale, A.; Li, X. A modeling and experimental study of capacity fade for lithium-ion batteries. *Energy AI* **2020**, *2*, 100032. [[CrossRef](#)]

51. Larsson, F.; Mellander, B.-E. Abuse by external heating, overcharge and short circuiting of commercial lithium-ion battery cells. *J. Electrochem. Soc.* **2014**, *161*, A1611. [[CrossRef](#)]
52. Ouyang, T.; Liu, B.; Wang, C.; Ye, J.; Liu, S. Novel hybrid thermal management system for preventing Li-ion battery thermal runaway using nanofluids cooling. *Int. J. Heat Mass Transf.* **2023**, *201*, 123652. [[CrossRef](#)]
53. Capasso, C.; Veneri, O. Experimental analysis on the performance of lithium based batteries for road full electric and hybrid vehicles. *Appl. Energy* **2014**, *136*, 921–930.
54. Ahmeid, M.; Muhammad, M.; Lambert, S.; Attidekou, P.S.; Milojevic, Z. A rapid capacity evaluation of retired electric vehicle battery modules using partial discharge test. *J. Energy Storage* **2022**, *50*, 104562. [[CrossRef](#)]
55. Thakur, A.K.; Prabakaran, R.; Elkadeem, M.; Sharshir, S.W.; Arici, M.; Wang, C.; Zhao, W.; Hwang, J.-Y.; Saidur, R. A state of art review and future viewpoint on advance cooling techniques for Lithium-ion battery system of electric vehicles. *J. Energy Storage* **2020**, *32*, 101771. [[CrossRef](#)]
56. Baghdadi, I.; Briat, O.; Delétage, J.-Y.; Gyan, P.; Vinassa, J.-M. Lithium battery aging model based on Dakin's degradation approach. *J. Power Sources* **2016**, *325*, 273–285. [[CrossRef](#)]
57. Zhang, P.; Liang, J.; Zhang, F. An overview of different approaches for battery lifetime prediction. *IOP Conf. Ser. Mater. Sci. Eng.* **2017**, *199*, 012134. [[CrossRef](#)]
58. Xu, B.; Oudalov, A.; Ulbig, A.; Andersson, G.; Kirschen, D.S. Modeling of lithium-ion battery degradation for cell life assessment. *IEEE Trans. Smart Grid* **2016**, *9*, 1131–1140. [[CrossRef](#)]
59. Rallabandi, S.; Issac Selvaraj, R.V. Advancements in Battery Cooling Techniques for Enhanced Performance and Safety in Electric Vehicles: A Comprehensive Review. *Energy Technol.* **2024**, *12*, 2301404. [[CrossRef](#)]
60. Chavan, S.; Venkateswarlu, B.; Prabakaran, R.; Salman, M.; Joo, S.W.; Choi, G.S.; Kim, S.C. Thermal runaway and mitigation strategies for electric vehicle lithium-ion batteries using battery cooling approach: A review of the current status and challenges. *J. Energy Storage* **2023**, *72*, 108569. [[CrossRef](#)]
61. Xu, J.; Guo, Z.; Xu, Z.; Zhou, X.; Mei, X. A systematic review and comparison of liquid-based cooling system for lithium-ion batteries. *ETransportation* **2023**, *17*, 100242. [[CrossRef](#)]
62. Zhang, X.; Li, Z.; Luo, L.; Fan, Y.; Du, Z. A review on thermal management of lithium-ion batteries for electric vehicles. *Energy* **2022**, *238*, 121652. [[CrossRef](#)]
63. Mitra, A.; Kumar, R.; Singh, D.K. Thermal management of lithium-ion batteries using carbon-based nanofluid flowing through different flow channel configurations. *J. Power Sources* **2023**, *555*, 232351. [[CrossRef](#)]
64. Wu, S.; Lao, L.; Wu, L.; Liu, L.; Lin, C.; Zhang, Q. Effect analysis on integration efficiency and safety performance of a battery thermal management system based on direct contact liquid cooling. *Appl. Therm. Eng.* **2022**, *201*, 117788. [[CrossRef](#)]
65. Deng, J.; Huang, Q.; Li, X.; Zhang, G.; Li, C.; Li, S. Influence mechanism of battery thermal management with flexible flame retardant composite phase change materials by temperature aging. *Renew. Energy* **2024**, *222*, 119922. [[CrossRef](#)]
66. Lin, Y.; Jia, Y.; Alva, G.; Fang, G. Review on thermal conductivity enhancement, thermal properties and applications of phase change materials in thermal energy storage. *Renew. Sustain. Energy Rev.* **2018**, *82*, 2730–2742. [[CrossRef](#)]
67. Sadeh, M.; Tousi, M.; Sarchami, A.; Sanaie, R.; Kiani, M.; Ashjaee, M.; Houshfar, E. A novel hybrid liquid-cooled battery thermal management system for electric vehicles in highway fuel-economy condition. *J. Energy Storage* **2024**, *86*, 111195. [[CrossRef](#)]
68. Guo, Z.; Wang, Y.; Zhao, S.; Zhao, T.; Ni, M. Investigation of battery thermal management system with considering effect of battery aging and nanofluids. *Int. J. Heat Mass Transf.* **2023**, *202*, 123685. [[CrossRef](#)]
69. Zhang, K.; Zhou, J.; Tian, T.; Kai, Y.; Li, Y.; Zheng, B.; Yang, F. Cycling-induced damage of silicon-based lithium-ion batteries: Modeling and experimental validation. *Int. J. Fatigue* **2023**, *172*, 107660. [[CrossRef](#)]
70. Speltino, C.; Di Domenico, D.; Fiengo, G.; Stefanopoulou, A. Experimental identification and validation of an electrochemical model of a lithium-ion battery. In Proceedings of the 2009 European Control Conference (ECC), Budapest, Hungary, 23–26 August 2009; IEEE: Piscataway, NJ, USA, 2019; pp. 1053–1058.
71. Ouyang, D.; Weng, J.; Chen, M.; Wang, J. Impacts of current rates on the degradation behaviors of lithium-ion batteries under over-discharge conditions. *J. Electrochem. Soc.* **2019**, *166*, A3432. [[CrossRef](#)]
72. Zhang, Z.; Ji, C.; Liu, Y.; Wang, Y.; Wang, B.; Liu, D. Effect of Aging Path on Degradation Characteristics of Lithium-Ion Batteries in Low-Temperature Environments. *Batteries* **2024**, *10*, 107. [[CrossRef](#)]
73. Baek, K.; Hong, E.; Cha, S. Capacity fade modeling of a lithium-ion battery for electric vehicles. *Int. J. Automot. Technol.* **2015**, *16*, 309–315. [[CrossRef](#)]

Disclaimer/Publisher's Note: The statements, opinions and data contained in all publications are solely those of the individual author(s) and contributor(s) and not of MDPI and/or the editor(s). MDPI and/or the editor(s) disclaim responsibility for any injury to people or property resulting from any ideas, methods, instructions or products referred to in the content.